Chapter-2

A Molecular Theory of the Nematic to Nematic Phase Transition in Strongly Polar Compounds.

2.1 Introduction

As described in the previous chapter, the nematic (N) liquid crystal is characterised by a long range orientational order of the long axes of the molecules without a long range positional order of their centres of mass (see section 1.2.1, chapter-1). The preferred axis of orientation in the nematic liquid crystal, called the *director*, is represented by the unit vector $\hat{\boldsymbol{n}}$. The extent of orientational order in a cylindrically symmetric nematic liquid crystal is given by the so-called *scalar* order parameter *S* defined as

$$S = \tfrac{1}{2}\langle 3\cos^2\theta_i - 1\rangle = \langle P_2(\cos\theta_i)\rangle \tag{2.1}$$

where θ_i is the angle between the long axis of the i^{th} molecule and the director, P_2 is the second Legendre polynomial and $\langle\ \rangle$ denote a statistical average. The order parameter takes a maximum value equal to 1 when all the rods are perfectly aligned and is zero when all the orientations of the long axes are equally probable *i.e.*, in the isotropic phase.

When heated, usually a nematic liquid crystal undergoes a transition to the isotropic liquid. Since the nematic liquid crystal differs from the isotropic liquid only in an orientational order, one would not normally expect any other variation in the transition sequence. However, such variations have been observed in some special cases. For example, as described in chapter-1, in case of compounds consisting of molecules with polar end groups, when the reentrant nematic liquid crystal is heated, it undergoes a transition to the SmA_d liquid crystal. In the present chapter, we consider an even simpler transition between two nematics without any change in the macroscopic symmetry of the medium. Indeed, such transitions are known even in the more disordered isotropic phase. For example, water, even though an isotropic liquid, due to complex hydrogen bond formation, is known to exhibit a liquid-liquid transition associated with a jump in the density [1] in its super cooled state.

Some liquid crystal compounds consisting of ***strongly polar*** molecules show the nematic-nematic (N-N) transition associated with a jump in the order parameter. Experimentally, the first example of the N-N transition was found in a binary mixture [2] of polar compounds DB_8ONO_2 and $DB_{10}ONO_2$ where, DB_nONO_2 denotes the homologues of *n*-alkyloxyphenyl-nitrobenzoyloxybenzoate. The transition was discovered by high resolution calorimetric (see figure 2.1a) and X-ray diffraction techniques. The X-ray measurements indicated a jump in the short range smectic like order associated with the N-N transition. In fact, in the temperature -concentration phase diagram, the N-N transition line appears as a continuation of the SmA_1-SmA_d transition line (see figure 2.1b). Hence the transition is denoted as N_1-N_d transition. Here, the suffix 'd' denotes *dimers* and the suffix '1' *monomers* (see section 1.5.2, chapter-1) characterising the short range order.

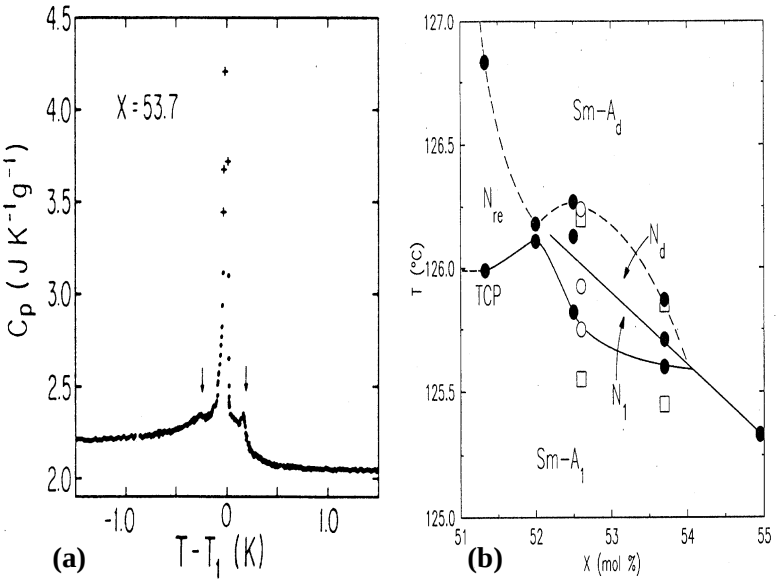

Figure-2.1. (a) Variation C_P for a sample with X = 53.7%, where X is the mole percent concentration of $DB_{10}ONO_2$ in DB_8ONO_2 [2a]. The strong peak in the middle corresponds to the N_d-N_1 transition and the small peak marked by the right arrow corresponds to SmA_d-N_d transition and the left arrow to SmA_1-N_1 transition. (b) Detail of the T-X phase diagram for the same mixture for X between 51% and 55% [2b]. Filled circles, open circles and open squares represent calorimetric, X-ray scattering and optical measurements respectively. The dashed curves indicate 2nd order phase transitions and the solid curves, 1st order ones. TCP marks the tricritical point.

The N_1-N_d transition has been subsequently observed in a single component system also [3]. In this experiment, the strongly polar compound *p*-cyanophenyl *p-n* heptylbenzoate (CP7B) contained in a *thin* cell was studied optically and a jump in the transmitted intensity indicating a jump in the orientational order parameter associated with the N_1-N_d transition was detected (see figure 2.2). Note that the N_1-N_d transition in this case is not associated with the smectic phase.

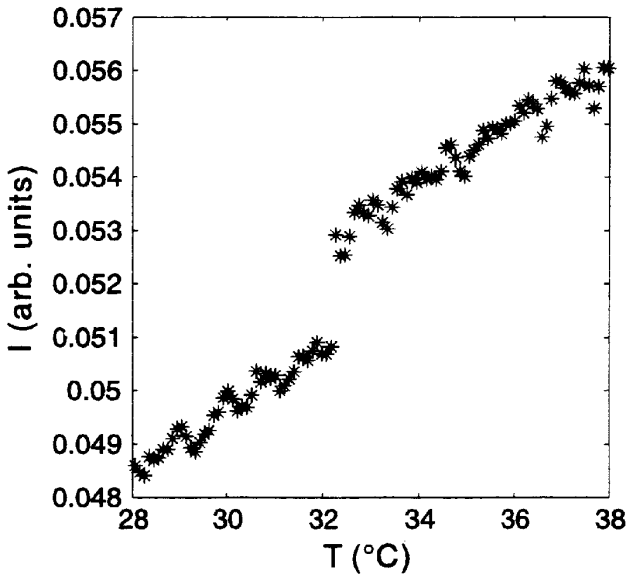

Figure-2.2. Variation in the transmitted intensity as a function of temperature for the compound CP7B for cell thickness of 1.9 μm [3]. Note the jump around 33^0 C.

As explained earlier (see section 1.5.2), the SmA-SmA transition is associated with a jump in the layer spacing. This has been successfully explained by the phenomenological theory developed by Prost [4, 5] using two coupled smectic order parameters corresponding to 'two competing lengths' (see section 1.6.4). This theory predicts the general phase diagrams showing the N_1-N_d transition as a continuation of the SmA-SmA transition line (see figure 2.3) in agreement with the experimental result of figure 2.1b [2]. Hence it is clear that the N_1-N_d transition is also associated with the two competing lengths characterising the short range smectic like order.

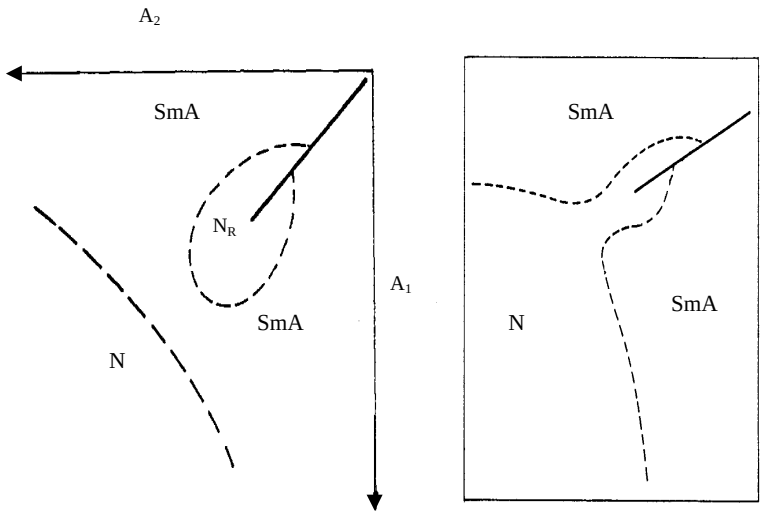

Figure-2.3. General phase diagrams predicted by the dislocation loop melting theory of Prost and Toner [4]. A_1 and A_2 are general variables which can be mapped to pressure and temperature or pressure and concentration etc.

A simple model to explain the molecular origin of the 'two lengths' assumed in the Prost's *phenomenological* model was proposed by Madhusudana and Jyothsna Rajan [6]. The basic concept in this model is that the molecular pairs can change over from anti-parallel (A) to parallel (P) configuration as the intermolecular separation (r) is reduced due to cooling or due to increase of pressure. The medium is treated as an equilibrium *mixture* of the A and P types of pairs. Recent experiments [7] showing the presence of *polar* short range order at low temperatures support this model. In this chapter, we extend this model to develop a *molecular* theory of the N_1-N_d transition. We begin with a description of this model.

2.2 Model for molecular pairs with parallel dipole moments at low temperatures

In the model proposed by Madhusudana and Jyothsna Rajan [6], the origin of the two incommensurate lengths is explained as follows: the permanent dipolar interaction favours an antiparallel arrangement between the neighbouring mesogenic molecules [8]. However, the aromatic part of the antiparallel neighbours overlap due

to the strong dispersion interaction between them leading to the partial bilayer arrangement (see figure 2.4a below and text in section 1.6.5 of chapter-1). In this configuration, the alkyl chains of the two molecules, which lie on opposite sides of the core region, do not have a significant interaction.

On the other hand, if the molecules are parallel, the permanent dipolar interaction is repulsive. However, the aromatic cores have strong polarizabilities and the induced dipole moment due to a neighbouring polar molecule would weaken the *net* dipole moment of any given molecule in this configuration (see figure 2.4b). Further, the chains of the two neighbours are now in close proximity and the dispersion interaction between them would favour this arrangement. The repulsive dipolar interaction is $\propto 1/r^3$ where r is the intermolecular separation, while both the dipole-induced dipole and the dispersion interactions are $\propto 1/r^6$ and are attractive in nature. Hence there can be a change from the antiparallel to the parallel configuration as the intermolecular separation is decreased below some value as the density is increased due to a lowering of temperature or an increase of pressure.

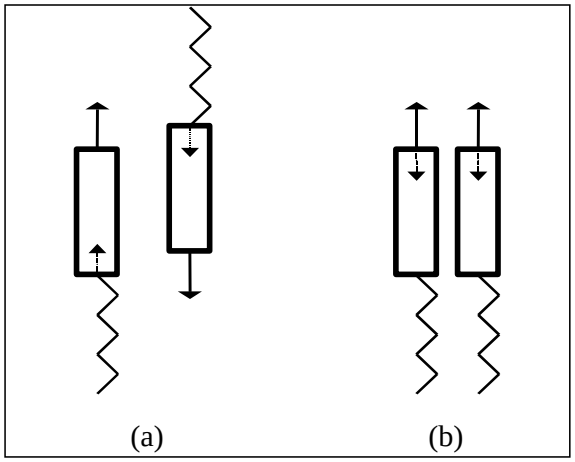

Figure-2.4. Schematic diagram showing (a) the antiparallel configuration of two molecules favoured at intermediate molecular separations and (b) the parallel configuration favoured at relatively low values of intermolecular separation. The arrow with a solid line represents the permanent dipole moment and the one with a dotted line, the induced one. (For the sake of clarity, the relative separation in (a) is exaggerated).

The following calculations show that the change over from the A-type configuration to the P-type configuration occurs for reasonable values of the

molecular parameters. Considering an antiparallel pair (see figure 2.4a), the induced dipole moment in a molecule is given by

$$\vec{p}_i = \chi \vec{\mathcal{E}} \tag{2.2}$$

where χ is the longitudinal component of the polarisability of the part of the core which is close to the dipole of the neighbour which generates an electric field $\vec{\mathcal{E}}$. We have, for short dipoles,

$$\vec{\mathcal{E}} = \frac{1}{4\pi\varepsilon_0}\frac{(\vec{p}+\vec{p}_i)}{r^3} \tag{2.3}$$

where ε_0 is the absolute permittivity of free space, $\vec{p}$ is the permanent dipole moment, $(\vec{p}+\vec{p}_i)$ is the *net* dipole moment of one of the molecules in the A-type configuration (see figure2.4a) and r is the intermolecular separation. From equations 2.2 and 2.3, we have

$$(\vec{p}+\vec{p}_i) = \frac{\vec{p}}{\left(1-\frac{\chi}{4\pi\varepsilon_0 r^3}\right)} \tag{2.4}$$

The pairing energy for an antiparallel pair is given by

$$E_A = -\frac{1}{4\pi\varepsilon_0}\frac{(p+p_i)^2}{r^3}$$

$$= -\frac{1}{4\pi\varepsilon_0 r^3}\frac{p^2}{\left(1-\frac{\chi}{4\pi\varepsilon_0 r^3}\right)^2} \tag{2.5}$$

For a P-type of pair (see figure 2.4b), the pairing energy is

$$E_P = +\frac{1}{4\pi\varepsilon_0 r^3}\frac{p^2}{\left(1+\frac{\chi}{4\pi\varepsilon_0 r^3}\right)^2} - \frac{Kc^2}{r^6} \tag{2.6}$$

where K is the chain-chain interaction parameter and c is the chain length. We do not explicitly include the energy due to the dispersion interaction between the cores as it is supposed to be the same in the A and P configurations.

To evaluate E_A and E_P, the following typical values [6] are used:

p = 4 Debye = 4/3 $5 10^{-29}$C m, $\chi/(4\pi\varepsilon_0)$ = 20 5 10^{-30} m^3, Kc^2 = 6.6 5 10^{-76} SI units. The pairing energy difference

$$\Delta E = E_A - E_P \tag{2.7}$$

is calculated for various values of r. A graph of ΔE against r is shown in figure 2.5. Note that the energy of two dipoles of strength 1D each separated by a distance of 1Å *i.e.,* $1D^2/Å^3$ in CGS units is equal to 10^{-19} J in SI units.

It can be seen that, for $r \leq 5.47$ Å, $\Delta E > 0$, *i.e.,* $E_P < E_A$ or the P-type configuration has lower energy than the A-type of configuration. This clearly shows that, as the intermolecular separation is decreased, the P-type configuration is favoured over the A-type configuration.

For simplicity, the above calculations are carried out restricting the interaction to two near neighbours. In the liquid crystal medium, many near neighbours interact. More than two molecules can have an all-parallel configuration, whereas many near neighbours can not be mutually antiparallel. In reference [6], as an example, molecules arranged in a two dimensional hexagonal lattice is considered for calculation of E_A, E_P and ΔE. The resulting graph of ΔE against r is very similar to that shown in figure 2.5.

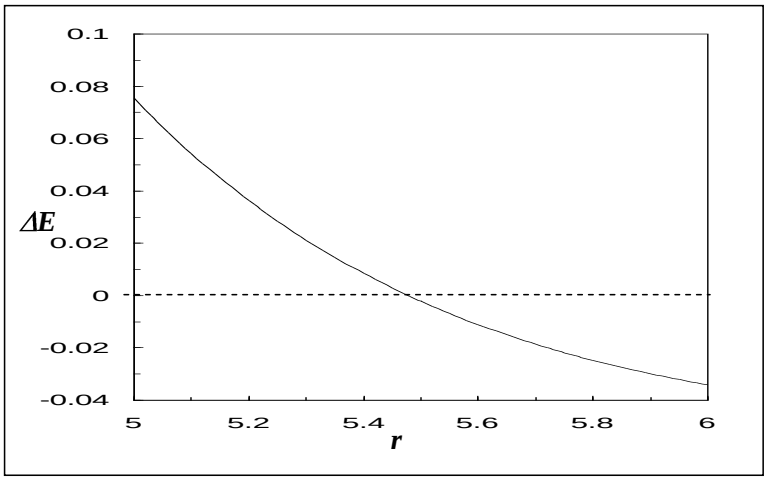

Figure-2.5. The pairing energy difference $\Delta E = E_A - E_P$ (in 10^{-19}J) between the antiparallel and parallel configurations plotted as a function of the intermolecular separation r (in Å).

Even though more than two near neighbours can have parallel configuration, for simplicity, as in reference [6], we consider the medium to be a mixture of A and P types of *pairs*. Incorporating these ideas, we develop a molecular theory for the nematic-nematic transition. For this, we extend the Maier-Saupe theory of nematic liquid crystals to develop a theory of nematic *mixtures*. In the next section we give a brief review of the Maier-Saupe theory.

2.3 Maier-Saupe theory for the N-I transition

Maier and Saupe (MS) [9] developed a molecular mean field theory of the nematic phase. In the theory, each molecule is assumed to be in an average orienting field due to its environment, but otherwise uncorrelated with its neighbours. MS assumed that the anisotropic dispersion forces are entirely responsible for the orientational order and ignored the shape anisotropy of the molecules. Using the mean field approximation, MS wrote the single particle potential for the i^{th} molecule as

$$U_i = -U_0 S P_2(\cos\theta_i) \tag{2.8}$$

where U_0 is an interaction parameter and S is the nematic order parameter defined in equation 2.1 above. The parameter U_0 depends on the structural details of the constituent molecules and the molar volume of the compound. The molar internal energy is given by

$$U = \frac{N}{2}\langle U_i\rangle = -\frac{N}{2}U_0 S^2 \tag{2.9}$$

where N is the Avogadro number and $\langle\ \rangle$ denote a statistical average. The factor (1/2) arises since each molecule is counted twice while finding the average. The molar entropy is

$$\mathcal{S} = -Nk_B\langle \ln f(\cos\theta)\rangle \tag{2.10}$$

where k_B is the Boltzmann constant and $f(\cos\theta)$ is the normalised orientational distribution function. The molar Helmholtz free energy is written as

$$F = U - T\mathcal{S} \tag{2.11}$$

The orientational distribution function found by minimising F is given by

$$f(\cos\theta) = Z^{-1}\exp(-U_i/k_B T) \tag{2.12}$$

where Z is the normalising integral. The orientational order parameter is calculated using

$$S = \int_0^1 \mathrm{d}(\cos\theta)\, f(\cos\theta) P_2(\cos\theta). \tag{2.13}$$

It can be verified that minimising the free energy with respect to S also leads to the same expression for S. Using equations 2.10 to 2.13, the free energy per particle can be written in the dimensionless form as

$$\frac{F}{Nk_BT} = + \frac{U_0}{2k_BT} S^2 - \ln Z. \tag{2.14}$$

For a given value of (U_0/k_BT), equation 2.13 is solved for self consistency and the free energy is calculated using equation 2.14. This represents the excess free energy over that of the isotropic phase, due to the onset of orientational order. Hence, the solutions resulting in $F<0$ correspond to the stable nematic phase. This procedure is repeated for different values of (U_0/k_BT). The nematic-isotropic transition occurs when the calculated free energy becomes zero. MS showed that the calculations lead to a first order N-I transition at $S_{NI} = 0.4292$ and found that

$$U_0/k_BT_{NI} = 4.541 \tag{2.15}$$

where T_{NI} is the N-I transition temperature.

We now extend the MS theory to develop the theory for nematic-nematic transition in strongly polar compounds.

2.4 Nematic-nematic transition in strongly polar compounds

2.4.1 Theoretical model

2.4.1.1 Assumptions

In order to simplify the calculations, the following assumptions are made.

(1) For the sake of simplicity and in view of our earlier discussions regarding the dependence of the mutual configuration of near neighbours on the intermolecular separation, we assume that the medium consists of pairs of molecules which have either an antiparallel (A) or parallel (P) configuration. In the former case, frustration

in the orientation of a third molecule can be expected to favour the formation of pairs. On the other hand, we may expect a large number of molecules to be associated in a P-type configuration. A statistical mechanical description of the latter becomes quite complex and for the sake of simplicity, we assume that even the P-type configurations have only effective *pairs*, as in the reference [6].

(2) As we described earlier, the A-type (P-type) configuration is favoured at lower (higher) densities. Hence, ΔE should be expressed as a function of density. Developing the model with such an expression requires the inclusion of hard rod features of the interactions as well as the effect of excluded volume. These are included in a hybrid model which is described in chapter-5. In the present calculations, for the sake of simplicity, the density and hence the intermolecular separation are assumed to be monotonic functions of temperature. Hence, as in reference [6], the energy difference between the two configurations is written in the following form:

$$\Delta E = E_A - E_P = R_1 k_B T_{NI}\left(\frac{R_2}{T_R} - 1\right) \tag{2.16}$$

where k_B is the Boltzmann constant, E_A and E_P are the configurational energies of the A-type and P-type pairs respectively, T_{NI} is the nematic-isotropic transition temperature of the A-type of pairs, $R_1 k_B T_{NI}$ is an interaction parameter and $T_R = T/T_{NI}$ is the reduced temperature. R_2 is the reduced temperature at which the density of the medium is such that ΔE becomes zero. For $T_R > R_2$, the A-type configuration has the lower energy.

(3) It is clear from figure 2.4 that the geometrical parameters of the two configurations are different. Hence we assume that the orientational potential for A-type of pairs (U_{AA}) and P-type of pairs (U_{PP}) to be different. We write,

$$U_{PP} = Y\, U_{AA} \tag{2.17}$$

and the mutual interaction potential

$$U_{AP} = U_{PA} = P\sqrt{U_{AA}\, U_{PP}}$$

$$= P\sqrt{Y}\, U_{AA} \tag{2.18}$$

where $P \neq 1$ indicates a deviation from the geometric mean (GM) approximation for the mutual interaction and $(P-1)$ is a measure of this deviation.

2.4.1.2 Expressions for the free energy and the order parameters

As mentioned earlier, the medium is assumed to consist of a *mixture* of A-type and P-type pairs. Following the method of Humphries *et al.* [10] for the mean field molecular theory of *mixtures*, we write the orientational potential energy for the i^{th} A-type pair as

$$U_{Ai} = -U_{AA} X_A S_A P_2(\cos\theta_{Ai}) - U_{AP} X_P S_P P_2(\cos\theta_{Ai}) \qquad (2.19)$$

where U_{AA} is the mean field interaction potential between A-type pairs, U_{AP} that between A-type and P-type pairs, X_A, X_p and S_A, S_P are the mole fractions and the orientational order parameters of the A and P types of pairs respectively and P_2 is the second Legendre polynomial.

Similarly for a P-type pair,

$$U_{Pj} = -U_{PP} X_P S_P P_2(\cos\theta_{Pj}) - U_{PA} X_A S_A P_2(\cos\theta_{Pj}) \qquad (2.20)$$

where U_{PP} is the interaction potential between P-type pairs and the mutual interaction potential $U_{PA} = U_{AP}$.

As usual, we have,

$$X_A + X_P = 1 \qquad (2.21)$$

We can now write the internal energy of one mole of *pairs* by averaging over the distribution functions as

$$2U = \frac{NX_A}{2}\langle U_{Ai}\rangle + \frac{NX_P}{2}\langle U_{Pj}\rangle - NX_P \Delta E$$

$$= -\frac{N}{2}[U_{AA} X_A^2 S_A^2 + U_{PP} X_P^2 S_P^2 + 2U_{AP} X_A X_P S_A S_P] - NX_P \Delta E \qquad (2.22)$$

where N is the Avogadro number, $\langle\ \rangle$ indicate statistical averages and the factor 2 on the left hand side reminds that we have a mole of pairs. The last term is the concentration dependent part of the configurational energy.

The molar entropy is given by

$$2\mathcal{S} = -N k_B [X_A \int d(\cos\theta_{Ai}) f_{Ai} \ln f_{Ai} + X_P \int d(\cos\theta_{Pj}) f_{Pj} \ln f_{Pj}]$$

$$- N k_B (X_A \ln X_A + X_P \ln X_P) \qquad (2.23)$$

where the last term is the entropy of mixing and f_A and f_P are the normalised distribution functions of A and P types of pairs respectively. The Helmholtz free energy is given by:

$$F = U - T\mathcal{S}. \tag{2.24}$$

The distribution functions f_A and f_P and also X_A are found by minimising F. The normalized orientational distribution functions of the A and P types of pairs are, respectively,

$$f_{Ai}(\cos\theta) = \frac{1}{Z_A}\exp(-U_{Ai}/k_BT) \tag{2.25}$$

$$f_{Pj}(\cos\theta) = \frac{1}{Z_P}\exp(-U_{Pj}/k_BT) \tag{2.26}$$

and

$$X_A = \frac{1}{1 + \frac{Z_P}{Z_A}\exp(\Delta E/k_BT)} \tag{2.27}$$

where Z_A and Z_P are the appropriate normalising integrals. The expressions for the order parameters are,

$$S_A = \langle P_2(\cos\theta_{Ai})\rangle = \int_0^1 d(\cos\theta_i)\, f_{Ai}(\cos\theta)P_2(\cos\theta_{Ai}) \tag{2.28}$$

$$S_P = \langle P_2(\cos\theta_{Pj})\rangle = \int_0^1 d(\cos\theta_j)\, f_{Pj}(\cos\theta)P_2(\cos\theta_{Pj}). \tag{2.29}$$

2.4.1.3 Specific heat at constant volume

The molar specific heat at constant volume is given by

$$C_V = \left(\frac{\partial U}{\partial T}\right)_V$$

$$= -\frac{NU_{AA}}{2}\left[\frac{\partial X_A}{\partial T}\{ X_A S_A^2 - YX_P S_P^2 + P\sqrt{Y}\ S_A S_P (X_P - X_A)\}\right.$$

$$+\frac{\partial S_A}{\partial T}\{ X_A^2 S_A + P\sqrt{Y}\ X_A X_P S_P\} + \left.\frac{\partial S_P}{\partial T}\{YX_P^2 S_P + P\sqrt{Y}\ X_A X_P S_A\}\right]$$

$$+\frac{\partial X_A}{\partial T} N\Delta E. \qquad (2.30)$$

where we have used equations 2.17 and 2.18. Note that in the above expression, we have not differentiated ΔE with respect to T. As we discussed in the introduction, ΔE is truly a function of intermolecular separation, or equivalently, the volume of the system. It is purely for the sake of convenience in calculation that ΔE is written as a function of temperature. As such in calculating C_V, in which the volume is held fixed, we do not differentiate ΔE with respect to temperature. Expressions for the derivatives of X_A, S_A and S_P are obtained by differentiating the relevant parameters in the equations 2.27, 2.28 and 2.29 respectively, with respect to T. We get,

$$\frac{\partial X_A}{\partial T}\left[\frac{U_{AA}}{k_B T}(- S_A^2 - YS_P^2 + 2P\sqrt{Y}\ S_A S_P) + \frac{1}{X_A X_P}\right]$$

$$+\frac{\partial S_A}{\partial T}\left[\frac{U_{AA}}{k_B T}(P\sqrt{Y}\ X_A S_P - X_A S_A)\right] + \frac{\partial S_P}{\partial T}\left[\frac{U_{AA}}{k_B T}(YX_P S_P - P\sqrt{Y}\ X_P S_A)\right]$$

$$+\frac{U_{AA}}{k_B T^2}[X_A S_A^2 - YX_P S_P^2 + P\sqrt{Y}\ S_A S_P (X_P - X_A)] - \frac{\Delta E}{k_B T^2} = 0. \qquad (2.31)$$

$$\frac{\partial X_A}{\partial T}\left[\frac{U_{AA}}{k_B T}(S_A - P\sqrt{Y} S_P)\right] + \frac{\partial S_A}{\partial T}\left[\frac{U_{AA}}{k_B T} X_A - \frac{1}{\Delta A}\right] + \frac{\partial S_P}{\partial T}\left[\frac{U_{AA}}{k_B T} P\sqrt{Y}\ X_P\right]$$

$$-\frac{U_{AA}}{k_B T^2}[X_A S_A + P\sqrt{Y} X_P S_P] = 0. \qquad (2.32)$$

$$\frac{\partial X_A}{\partial T}\left[\frac{U_{AA}}{k_B T}(P\sqrt{Y}S_A - YS_P)\right] + \frac{\partial S_A}{\partial T}\left[\frac{U_{AA}}{k_B T} P\sqrt{Y}\ X_A\right] + \frac{\partial S_P}{\partial T}\left[\frac{U_{AA}}{k_B T} YX_P - \frac{1}{\Delta P}\right]$$

$$-\frac{U_{AA}}{k_B T^2}[YX_P S_P + P\sqrt{Y} X_A S_A] = 0. \qquad (2.33)$$

where, we have used,

$$\Delta A = \langle [P_2(\cos\theta_A)]^2 \rangle - S_A^2$$

$$\text{and} \qquad \Delta P = \langle [P_2(\cos\theta_p)]^2 \rangle - S_p^2. \qquad (2.34)$$

The relevant derivatives are obtained by solving the three simultaneous equations 2.31, 2.32 and 2.33 and hence C_V is calculated.

2.4.2 Method of calculation

All the temperatures are referred to the N-I transition temperature of the A-type of pairs *i.e.*, we use the reduced temperature $T_R = T/(T_{NI})_A$. The parameter U_{AA} is eliminated using the MS condition given by equation 2.15 with $(T_{NI})_A$, *i.e.*, we write $U_{AA}/k_B(T_{NI})_A = 4.541$. The four independent parameters of the model are R_1, R_2, Y and P. We have used $R_2 = 0.6$. The value of R_1 is estimated as follows. For $T_R \approx 0.55$, we have from equation 2.16, $\Delta E = 0.1\times R_1 k_B T_{NI}$. Taking $T_{NI} = (T_{NI})_A = 500$K, we get $\Delta E \approx R_1\times 7\times 10^{-22}$ J. At $T_R \approx 0.55$, if the intermolecular separation r is taken to be 5Å, then, from figure 2.5, we have $\Delta E \approx 0.1\times 10^{-19}$ J. Hence, we take $R_1 = 15$. We use values of Y between 0.8 and 2, and P between 0.5 to 1. The significance of $Y\neq 1$ and $P\neq 1$ will be discussed in the next section. At any reduced temperature T_R, for the assumed set of the four parameters of the problem, consistent values of S_A and S_p are found using equations 2.28 and 2.29 for each X_A which is varied from 0 to 1. The free energy is calculated in each case. Near the minimum of F with respect to X_A, equation 2.27 is used to find the consistent value of X_A. We usually get more than one set of self consistent values of X_A , S_A and S_p. The stable solution corresponds to the one with the lowest value of F. Equation 2.24 gives the free energy of the nematic phase (F_N) with $S_A \neq 0$ and $S_p \neq 0$. Note that in the isotropic phase, $S_A = S_p = 0$, $Z_A = Z_P = 1$ (see equations 2.25 and 2.26) while in general $X_A \neq X_P$ (see equation 2.27). Hence, equation 2.24 gives the free energy of the isotropic phase (F_I) with $S_A = S_P = 0$. The nematic phase is stable if $\Delta F = F_N - F_I$ is negative. The average orientational order parameter is calculated as

$$\bar{S} = X_A S_A + X_P S_P \tag{2.35}$$

The necessary integrals have been evaluated numerically using a 32 point Gaussian quadrature method in double precision. In the next section, we present the results and compare them with experiments and other theoretical models.

2.4.3 Results and discussion

2.4.3.1 First order N_1-N_d transition ending in a critical point

We denote the nematic phase with a relatively larger value of X_A as the N_d phase and the one with a relatively smaller value of X_A as the N_1 phase. Since the N_1 and the N_d phases have the same symmetry, we can expect a first order N_1-N_d transition or a continuous evolution of N_1 to N_d beyond a critical point. For some values of the model parameters and in a *narrow* range of temperatures, the free energy has *two* minima with respect to X_A. The presence of two minima indicates the existence of two different nematic phases with different values of X_A. Indeed, by a careful numerical calculation we find that, at some temperature, the two minima in the free energy become equal. This implies a first order transition between the two nematic phases associated with a jump in X_A. We illustrate this trend for Y =1.4 in figure 2.6. Note that the calculations are made in a very narrow range of T_R values and it is rather easy to miss this transition in the calculations.

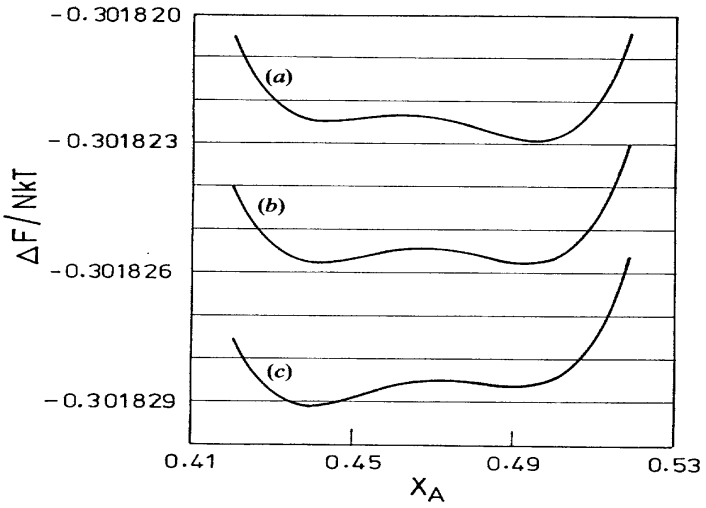

Figure-2.6. Molar Helmholtz free energy difference $\Delta F = F_{nematic} - F_{isotropic}$ plotted as a function of the relative concentration of the A-type of pairs (X_A) for Y = 1.4 and P = 0.6954, at three temperatures near the N_1-N_d transition point, (*a*) T_R = 0.62659436 at which the N_d phase has lower free energy, (*b*) T_R = 0.62659386 at which the free energy of the N_d phase is equal to that of the N_1 phase and (*c*) T_R = 0.62659340 at which the N_1 phase has a lower free energy.

Sine the N_1-N_d transition is a result of the change of the pair configuration from P-type to A-type, naturally we can expect the transition to take place at $T_R \approx R_2$. Indeed, for $Y \approx 1$, we get the N_1-N_d transition at $T_R \approx 0.6$, for $P < 0.573$.

We have found that a significant *negative* deviation from the geometric mean (GM) approximation for the mutual interaction (*i.e.,* $P < 1$ in equation 2.18) is *necessary* to get the N_1-N_d transition. The significance of the negative deviation will be discussed in the next subsection. As the deviation becomes smaller (*i.e.,* as P is increased keeping all other parameters fixed), the jump in X_A decreases, until a critical point is reached beyond which there is no phase transition separating the two nematic phases (see figure 2.7).

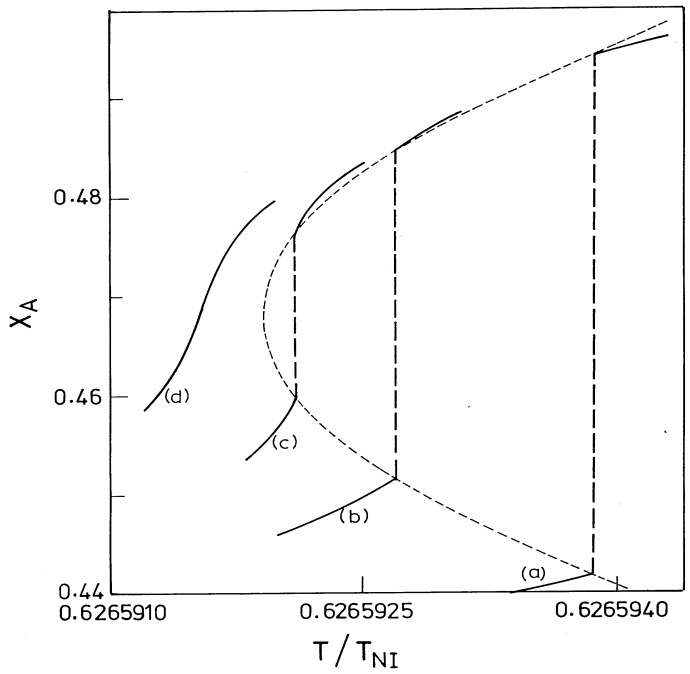

Figure-2.7. Relative concentration of the A-type of pairs (X_A) plotted as a function of the reduced temperature T/T_{NI} for Y = 1.4 for different values of P. (a) P = 0.6954, (b) P = 0.6956, (c) P = 0.6957, (d) P = 0.6958.

We have also evaluated the heat of the N_1-N_d transition (*i.e.,* ΔU, see figure 2.8). The transition is found to be very much weaker than the N-I transition. In the range of our calculations, the highest heat of transition is ~ 50joule/mol, *i.e.,* an order of magnitude smaller than the corresponding value at the N-I transition. Consequently,

the specific heat shows a strong peak as the transition point is approached from either side (see figure 2.9) as in the experimental diagram (figure 2.1a). As the critical point is approached, the sharpness of the peak increases further. We have shown the temperature variations of the order parameters S_A, S_P and $\overline{S}$ near the N_1- N_d transition point in figures 2.10 to 2.12 respectively. Since X_A has a positive jump at the N_1- N_d transition, the corresponding jump in S_A is positive while that in S_P is negative. However, note that $S_P > S_A$ since we have used $Y>1$. Thus the variation of $\overline{S}$ is similar to that of S_P. The diagram showing the jump in S_A resembles the trend in the experimental diagram shown in figure 2.2. For the sake of comparison, we have plotted in figure 2.13 jumps in the various parameters like X_A, S_A, S_P, $\overline{S}$ and $\tilde{U} = 2U/(Nk_BT)$ as functions of P for Y =1.4. All these jumps decrease continuously to zero as P approaches $P_{cr} \approx 0.69573$.

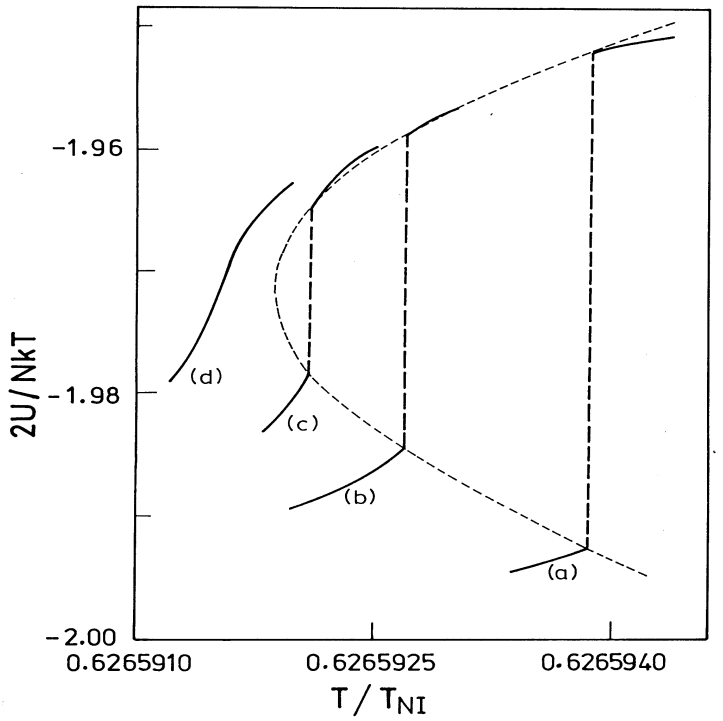

Figure-2.8. Internal energy per mole of pairs ($2U$) plotted as a function of T/T_{NI} for Y = 1.4, for different values of P. (a), (b), (c) and (d) have the same significance as in figure 2.7.

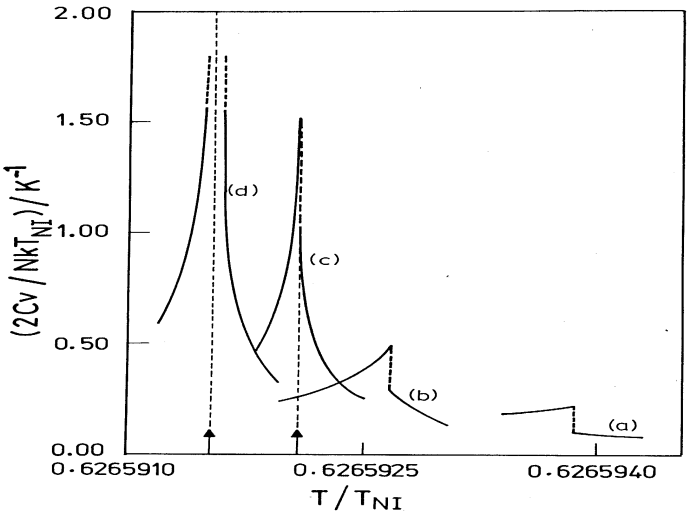

Figure-2.9. Specific heat at constant volume per mole of pairs ($2C_v$) plotted as a function of T/T_{NI} for Y = 1.4, for different values of P. (a), (b), (c) and (d) have the same significance as in figure 2.7.

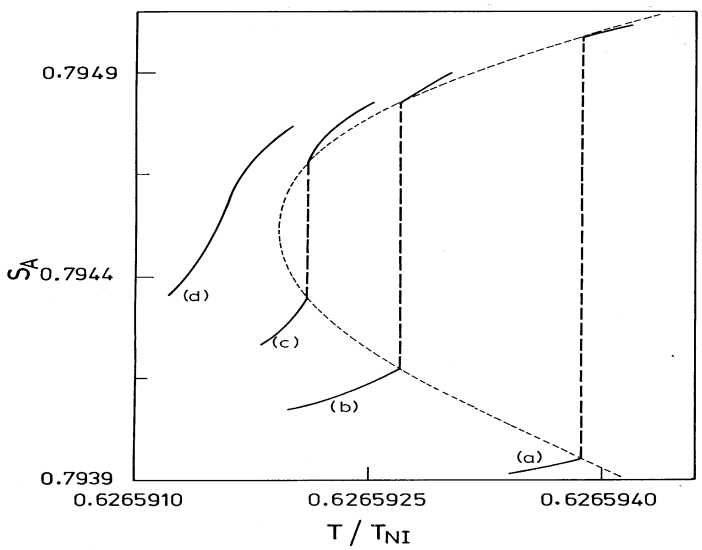

Figure- 2.10. Order parameter of the A-type of species (S_A) plotted as a function of T/T_{NI} for Y = 1.4, for different values of P. (a), (b), (c) and (d) have the same significance as in figure 2.7.

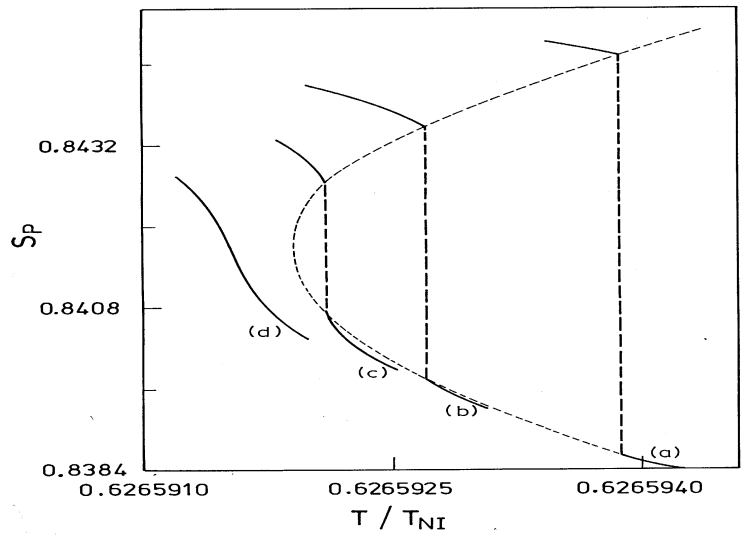

Figure-2.11. Order parameter of the P-type of species (S_P) plotted as a function of T/T_{NI} for Y = 1.4, for different values of P. (a), (b), (c) and (d) have the same significance as in figure 2.7.

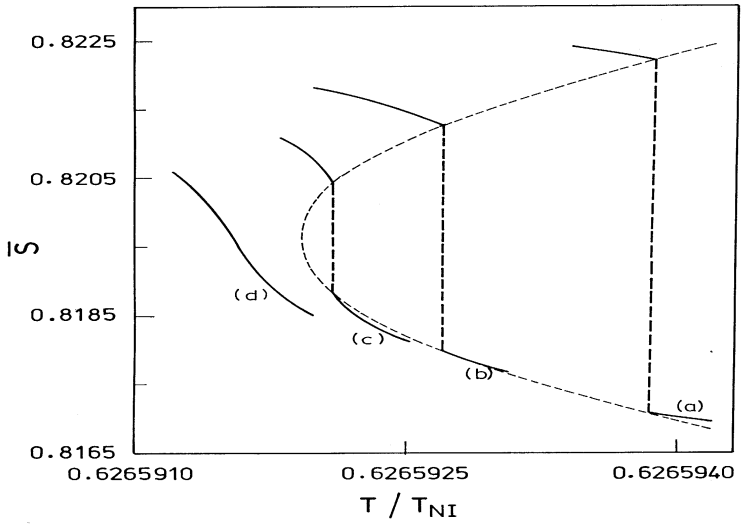

Figure-2.12. Averaged order parameter ($\bar{S}$) plotted as a function of T/T_{NI} for Y = 1.4, for different values of P. (a), (b), (c) and (d) have the same significance as in figure 2.7.

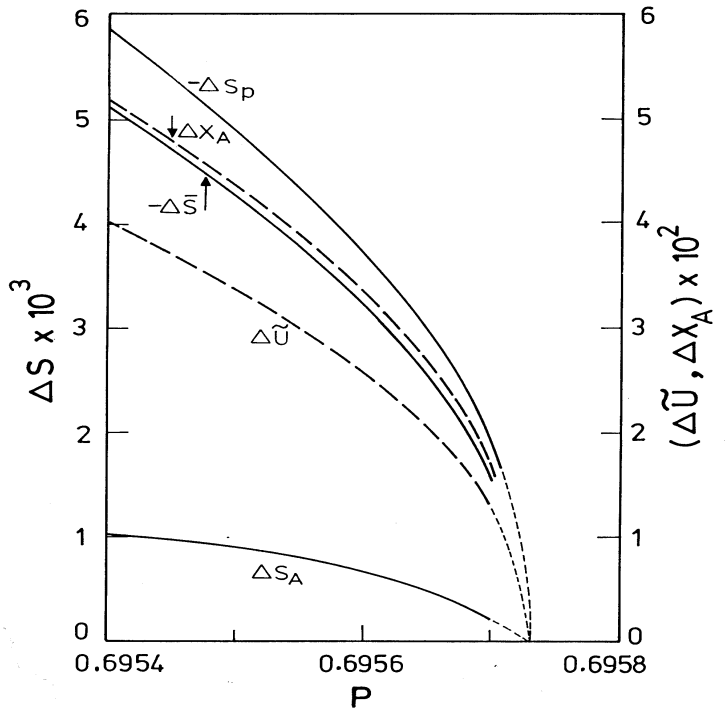

Figure-2.13. Variations of the jumps in X_A, S_A, S_P, $\bar{S}$ and $\tilde{U} = 2U/(Nk_BT)$ at the N_1-N_d transition point as functions of P for $Y = 1.4$. Note that the jumps in S_P and $\bar{S}$ are negative. The jumps decrease continuously to zero as P approaches $P_{cr} = 0.69573$. The light dashed lines are etrapolated from lower P values.

2.4.3.2 Significance of negative deviation from the GM approximation

It is interesting to compare these results on N_1-N_d transition with some earlier models of the N-I transition. As in most theories of mixtures, Humphries *et al.*[10] used the well-known geometric mean approximation for the mutual interaction (*i.e*, $P = 1$ in equation 2.18), since it is mathematically convenient and can be justified if only the dispersion interaction is relevant. In most binary mixtures of nematogens, the N-I transition curve is concave towards the isotropic phase in the temperature - concentration phase diagram. In other words, the N-I transition temperatures of the mixtures have a negative deviation from the linear dependence on the relative concentration. Humphries and Luckhurst [11] have shown that, these results can be

theoretically explained by assuming that the mutual attractive interaction between the two components is *less* than that given by the geometric mean value of the interaction energies of the pure components. Also, a comparison with the experimental data shows that this negative deviation from the GM approximation increases as the molecular structures of the two components become more dissimilar [11]. Later, Nakagawa and Akahane [12] have extended the molecular mean field theory of nematic mixtures developed by Humphries *et.al.* [10], by introducing an effective repulsive potential which depends on the average excluded volume. They have shown that, even if the GM approximation is assumed to hold good for the *attractive* part of the mutual interaction, the concave shape of the N-I transition curve naturally follows from the *hard core* interactions. In fact, assuming the GM approximation to hold good, hard rod theories of mixtures of rods with two different length to breadth ratios [12, 13, 14] give rise to phase boundaries which would correspond to $P < 1$ in the context of the theory of Humphries *et al* [10].

Palffy-Muhoray *et al.* [15] have extended the Humphries *et al.* model by taking into account the volume dependence of the potential functions. Apart from getting a nematic-isotropic coexistence range, they have also found a nematic-nematic *coexistence* at sufficiently low temperatures when the T_{NI} values of the two components differ considerably. Indeed, experiments on mixtures of two very dissimilar chemical species have shown such a *coexistence* [16, 17] of two nematic phases. However, due to the shape factor alone, the N_1-N_d *transition* is not found either theoretically or experimentally.

In chapter-5, we develop a hybrid model including the hard rod features of the interactions and get the N_1-N_d transition *without* assuming any deviation from the GM approximation for the attractive interaction *i.e.*, the hard rod effects alone are sufficient to give rise to the N_1-N_d transition. We also show in chapter-5, in agreement with Nakagawa *et.al.* [12], that neglecting the hard core interaction is equivalent to a negative deviation in the geometric mean approximation for the effective mutual *attractive* interaction between A and P types of pairs and this deviation increases as the two components become structurally more dissimilar. In our present calculations, the medium is assumed to be a *mixture* of A and P types of pairs and the hard rod effects have not been taken into account. Hence, the *negative* deviation from the GM approximation reflects the excluded volume effects.

2.4.3.3 Effect of variation of the parameter Y:

Since the P-type of pairs are shorter than the A-type of pairs, we may expect that $U_{PP} < U_{AA}$ *i.e.*, $Y < 1$ (see equation 2.17). In this case, the P-type component will have a lower T_{NI} value than the A-type component. However, as we discussed in the introduction, the A-type configuration may actually occur as pairs due to frustration effects. The frustration effect may also effectively reduce the orientational potential between the neigbouring A-type pairs. On the other hand, the P-type configuration should favour the formation of large clusters which can enhance the orientational potential of the effective pairs used in our model. Thus, even though the P-type configuration is favoured to occur at lower temperatures, it is quite possible that the orientational potential U_{PP} may be considerably higher than U_{AA} of the A-type species, which are favoured to occur at higher temperatures. This is equivalent to taking $Y > 1$ in equation 2.17. Hence, we have carried out the calculations for $Y \approx 1$ and also for $Y > 1$.

When Y= 0.9, we get $P_{cr} \approx 0.531$. When Y= 0.999, P_{cr} increases to about 0.5732. When $Y > 1$, we get the N_1-N_d transition for still higher values of P. For example, when $Y=2$, $P_{cr} \approx 0.82$. The increase of P_{cr} with Y can be interpreted as follows.

For a given value of Y, we have $U_{AP} \propto P$ (see equation 2.18). When $P < P_{cr}$, U_{AP} is sufficiently low to make the 'middle' values of X_A relatively less favoured. This causes a 'hump' in the variation of the free energy (F) with respect to X_A at $X_A \approx 0.5$ resulting in two minima in F as in figure 2.6. As mentioned earlier, the N_1-N_d transition occurs at a temperature (T_{NN}) at which these two minima have equal values (see figure 2.6). As the N_1-N_d critical point is approached, *i.e.*, as P is increased, U_{AP} becomes larger, the hump in the free energy decreases and finally vanishes at $P=P_{cr}$. As $U_{PP} \propto Y$ and $U_{AP} \propto P\sqrt{Y}$ (see equations 2.17 and 2.18), if Y is increased, U_{AP} grows more slowly than U_{PP}. Therefore, in the variation of F vs X_A, the minimum with smaller value of X_A becomes deeper than the other minimum, *i.e.*, N_1 phase becomes stable as in figure 2.6(c) and T_{NN} increases. To make the hump vanish again, a higher value of P_{cr} is required. It can be seen from figure 2.14 that, P_{cr} varies roughly linearly with $\sqrt{Y}$ for higher values of Y.

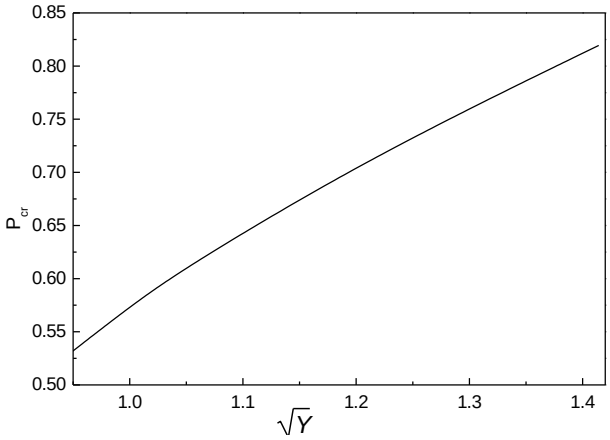

Figure -2.14. The critical value of *P* plotted as a function of $\sqrt{Y}$.

Irrespective of the value of Y, the N_1-N_d critical point is approached as P is increased. On the other hand, the variation of T_{NN} with respect to P depends on the value of Y. For $Y = 1$, $U_{AA}=U_{PP}$, and X_A, S_A, S_P values in the N_1 phase are the same as X_P, S_P, S_A respectively in the N_d phase. This makes $\overline{S}$ independent of X_A and there is no jump in $\overline{S}$ at the transition. Also, $T_{NN}/T_{NI} = R_2=0.6$, and does not vary with P. For $Y>1$, the P-type pairs are more favoured than the A-type pairs leading to $T_{NN}/T_{NI}>R_2$, *i.e.*, as Y is increased, X_A decreases. For example, in figure 2.15(d), at the critical point, $X_A\approx0.54$ for $Y=0.9$, whereas $X_A\approx0.47$ for $Y=1.4$ in figure 2.7(d). Therefore, a decrease in the value of $P(<P_{cr})$ with $Y>1$ leads to a greater stability of the N_1 phase. To bring about the N_1-N_d transition, a higher value of T_{NN} is required. This trend is seen, for example in figure 2.7 (d) to (a). On the other hand, for $Y<1$, the trend is opposite as seen in figure 2.15 (d) to (a). Also, a decrease in the value of Y decreases both U_{PP} and U_{AP}. Thus, $\overline{S}$ at the critical point decreases with Y as can be seen from figures 2.12(d) and 2.16(d). Note that, with $Y=0.9$, as the *temperature* is increased, the average order parameter $\overline{S}$ *increases* in a small range of temperatures near the N-N transition (figure 2.16). We have calculated $\overline{S}$ over a wider range of temperatures to verify that, away from T_{NN}, $\overline{S}$ decreases in general as the temperature is increased. The variation of $\overline{S}$ with temperature is shown in figure 2.17 for $Y=1.4$ and 0.9.

Experimentally it is found that the jump shown in figure 2.2 corresponds to a downward jump in $\bar{S}$ as the temperature is increased. This suggests that, it is reasonable to take $Y > 1$ in equation 2.17, as was argued earlier.

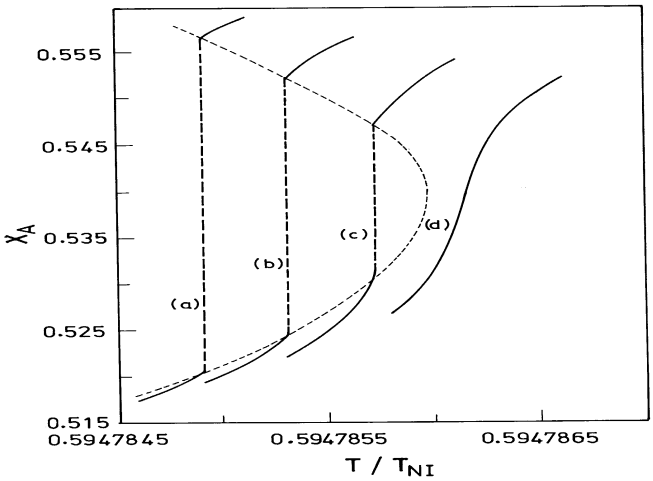

Figure-2.15. Relative concentration of the A-type of pairs (X_A) plotted as a function of the reduced temperature T/T_{NI} with Y = 0.9 for different values of P. (a) P = 0.5307, (b) P = 0.5308, (c) P = 0.5309, (d) P = 0.5310.

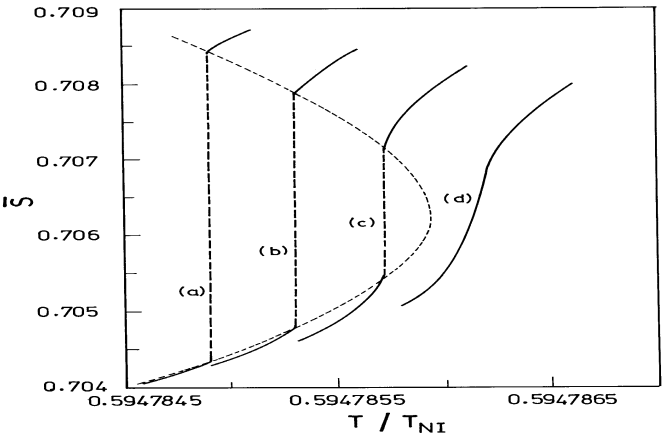

Figure-2.16. The jump in $\bar{S}$ plotted as a function of the reduced temperature T/T_{NI} for Y = 0.9 and different values of P. (a), (b), (c) and (d) have the same significance as in figure 2.15.

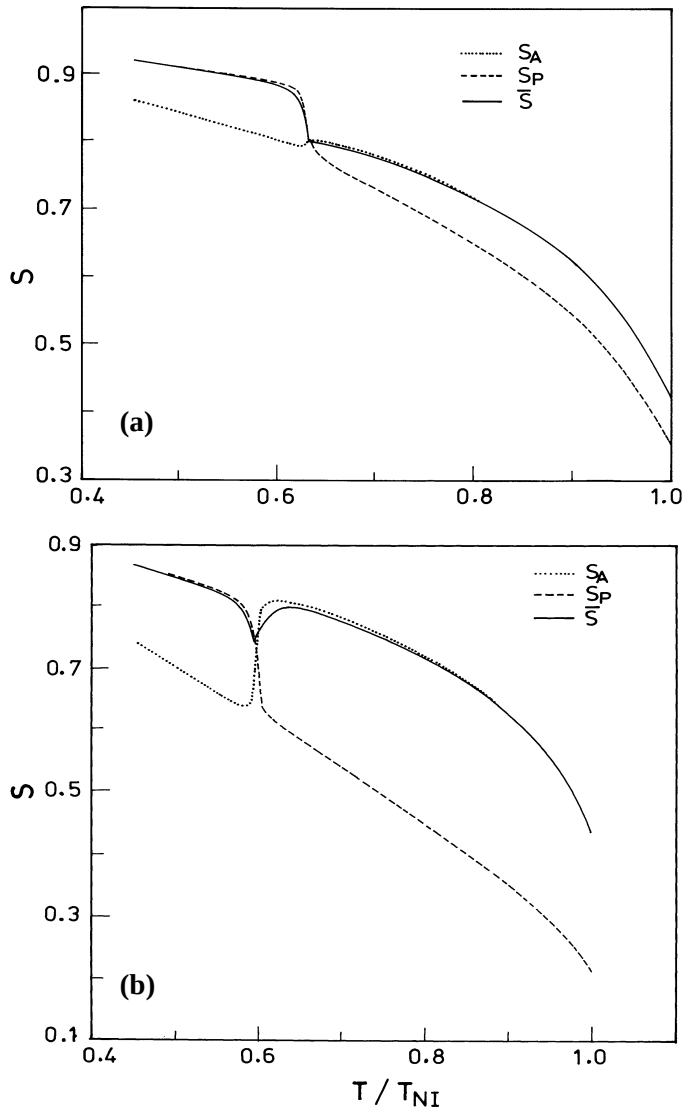

Figure-2.17. Variation of S_A, S_P and $\bar{S}$ plotted as a function of the reduced temperature T/T_{NI} over a wider range of temperatures for (a) Y =1.4 and P = 0.695 which is just below P_{cr} and (b) Y =0.9 and P = 0.53

2.5 Conclusions

A simple molecular theory of strongly polar compounds has been proposed by Madhusudana and Jyothsna Rajan to explain the phenomenon of double reentrance exhibited by such compounds. We have extended it to develop a molecular theory of the nematic-nematic (N_1-N_d) transition. We assume the medium to be a *mixture* of *pairs* having either parallel (P) or antiparallel (A) near neighbour configurations. We have extended the Maier-Saupe theory of nematic liquid crystals to develop a theory of such mixtures. We have shown that the N_1-N_d transition is a weak first order transition and which disappears above a critical point [18]. The N_1-N_d transition is associated with a jump in the relative concentration of the A and P types of pairs. We have also calculated the specific heat anomaly around the transition region. Usually, the effective mutual interaction between the two different species in a mixture is assumed to be the geometric mean of the interaction of the pure species. The consequence of a deviation from this approximation is discussed. We have shown that a *negative* deviation from the geometric mean approximation is required to get the N_1-N_d transition. The theoretical results are discussed in comparison with the available experimental data. In the next chapter, we extend the model to include the layering interactions and develop a model describing the smectic liquid crystals.

2.6 References for chapter-2

[1] Stanley, H. E., *Pramana*,**53**, 53,1999 and references there in.

[2] (a) Nounesis, G., Garland, C.W, and Shashidhar, R., *Phy. Rev. A*, **43**, 1849,1991, (b)Nounesis, G., Kumar, S., Pfeiffer, S., Shashidhar, R., and Garland, C.W, *Phy. Rev. Lett*, **73** , 565, 1994.

[3] Sobha. R. Warrier, Vijayaraghavan, D., and madhusudana, N.V., *Europhysics Lett*, **44**(3), 296,1998.

[4]deGennes, P.G., and Prost, J., *The Physics of liquid crystals*, 2nd edition, Clarendon press, Oxford, 1993.

[5] Prost, J., and Toner, J., *Phy. Rev. A*, **36**, 5008,1987.

[6] Madhusudana, N. V., and Jyothsna Rajan, *Liq.Cryst.*, **7**, 31, 1990.

[7] Basappa, G., and Madhusudana, N.V., *Eur. Phys. Journal B*, **1**, 179, 1998.

[8]Madhusudana . N . V and Chandrasekhar. S., *Pramana Suppl.*, **1**,57, 1973.

[9] Maier, W., and Saupe, A., *Z.Naturforsch*, **A14**, 882, 1959.

[10] Humphries, R. L., James, P. G., and Luckhurst, G. R., *Symp. Faraday Soc.*, **5**, 107, 1971.

[11] Humphries, and Luckhurst, G. R., *Chem. Phys. Lett.*,**23**, 567, 1973.

[12] Nakagawa, M., and Akahane, T., *J. Phys. Japan.*, **52**, 2659, 1983, *ibid*, **54**, 69, 1985.

[13] Counsell, C., and Warner, M., *Mol.Cryst.Liq.Cryst*., **100**, 307, 1983.

[14] Wagner, W, *Mol.Cryst.Liq.Cryst*., **98**, 247, 1983.

[15] Palffy-Muhoray, P., de Bruyn, J. J., and Dunmur, D. A., *Mol.Cryst.Liq.Cryst*., **127**, 301, 1985.

[16] Casagrande, C., Veyssie, M., and Finkelmann, H., *J. Phys. Lett., Paris*, **43**, L-671, 1982.

[17] Prathibha, R., and Madhusudana, N. V., *Mol.Cryst.Liq.Cryst. Lett*, **1**, 111, 1985.

[18] Govind, A. S., and Madhusudana, N. V., *Liq. Cryst*., **14**, 1539, 1993.

Formatted